



Modeling the tide and wind-induced circulation in Buzzards Bay

S. Sankaranarayanan

Applied Science Associates, 70, Dean Knauss Drive, Narragansett, RI-02882, United States

Received 1 August 2005; accepted 21 December 2006

Abstract

Hydrodynamic model application to Buzzards Bay is performed using a three-dimensional Boundary-fitted Hydrodynamic model in this study. The model is forced with observed tidal harmonic constants along the open boundaries and winds on the surface. The main focus of the present study is to model the detailed wind and tide-induced circulation in Buzzards Bay. The observed surface elevations and currents given in [Butman, B., Signell, R., Shoukimas, P., Beardsley, R.C., 1988. Current Observations in Buzzards Bay, 1982-1986. Open File Report 88-5 1988, United States Geological Survey] and the tide and current harmonics given in [Signell, R.P., 1987. Tide- and Wind-forced Currents in Buzzards Bay, Massachusetts. Technical Report WH-87-15 1987. Woods Hole Oceanographic Institution, Woods Hole, Massachusetts] are used to validate the model predictions. The calibrated model is then used to study the relative contributions of tidal and wind forcing on the instantaneous and residual circulation in Buzzards Bay. The amplitudes and phases of the principal tidal constituents at 10 tidal stations in Buzzards Bay obtained from a harmonic analysis of a 60-day simulation compare well with the observed data. The predicted amplitude and phase of the M_2 tidal constituent of surface elevations at these stations are, respectively, within 4 cm and 5° of the observed data. The errors in the model-predicted M_2 harmonic principal current speeds are less than 6 cm/s, and the principal current directions and phases are within 14° of the observations. The observed surface elevations and currents given in [Butman, B., Signell, R., Shoukimas, P., Beardsley, R.C., 1988. Current Observations in Buzzards Bay, 1982-1986. Open File Report 88-5 1988, United States Geological Survey] are used to validate the model-predicted low-frequency surface elevations and currents. The model predictions in low-frequency surface elevations at Woods Hole closely follow the trends seen in the observations with a correlation coefficient of 0.735, but fail to capture some of the peak surges seen in the observations. The model-predicted low-frequency currents in the east–west direction at stations in Buzzards Bay compare well with the observations with the correlation coefficient exceeding 0.811 and the model capturing the trends seen in the observations, for the most part. However, the model-predicted north–south velocities does not compare well with the observations. The model-predictions agree with the observations that the tidal currents in Vineyard Sound lagged the currents in Buzzards Bay by more than 3 h. The interaction of wind stress with large bathymetric gradients was shown to cause many vortices in Buzzards Bay, as seen from the model predictions. Model simulations show that the winds play a more dominant role than the tides in the generation of the barotropic residual currents in Buzzards Bay, while the model-predicted tide-induced residual current was seen to be small.

© 2007 Published by Elsevier Ltd.

1. Introduction

Buzzards Bay is an embayment located in the southeastern Massachusetts (Fig. 1). Buzzards Bay extends southwestward from the west end of Cape Cod Canal, opening into Rhode Island Sound at its mouth, and bounded to the southeast by Elizabeth Islands (Signell, 1987; Butman et al., 1988). Redfield (1953) investigated the tidal phenomena in Buzzards Bay and

Vineyard Sound by modeling the tidal elevations at a given point as the interference of two damped progressive waves traveling in opposite directions. The natural period of the bay (2 h) is substantially less than the dominant tidal period (12.4 h), so that the bay is in near equilibrium with the shelf tide. Redfield also argued that Vineyard Sound behaves like a strait, with the tidal wave from the Gulf of Maine to the east interfering with the wave from the New England shelf to the southwest, causing rapid changes in phase and tidal range.

An elaborate measurement of tides and currents in Buzzards Bay was performed during 1984–1985 by Butman

E-mail address: sankar@appsci.com

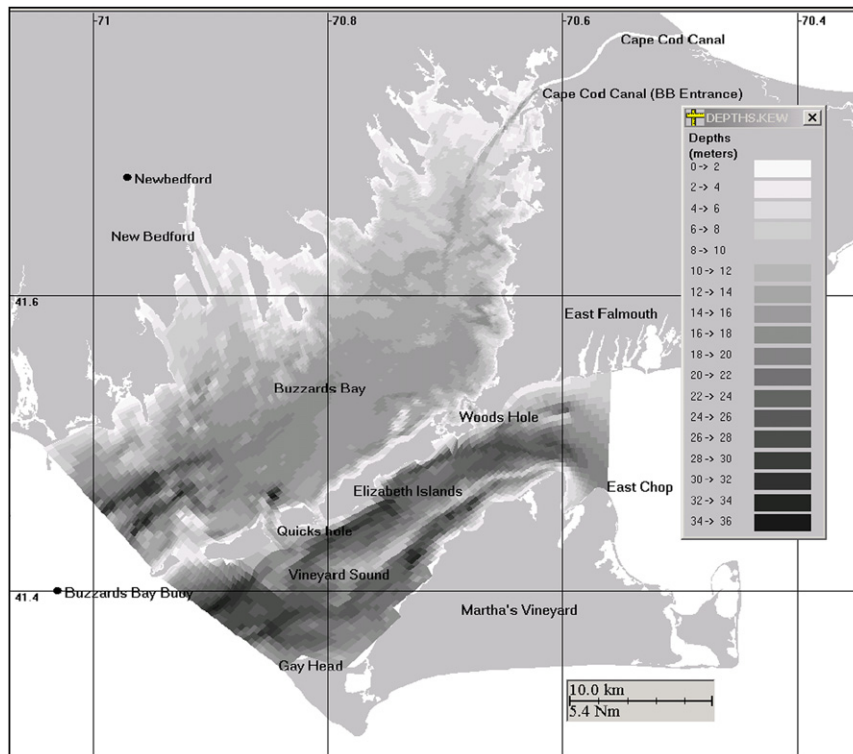


Fig. 1. The study area and its bathymetry.

et al. (1988) and this study remains the single best source of available current and elevation data in Buzzards Bay. Signell (1987) studied the residual flow field in Buzzards Bay using a nonlinear barotropic tidal model, based on a numerical scheme given by Flather and Heaps (1975). Although, Signell compared the observed and predicted residual flow field, a comparison of the observed and predicted tides and currents was not undertaken. Signell concluded that transport of material in the bay should be due to a combination of local response to winds and tide-induced dispersion caused by the small-scale residual field.

In the present study, three-dimensional Boundary-fitted Hydrodynamic model developed by Muin and Spaulding (1997a,b) is used to study the three-dimensional circulation induced by tides and winds. The main focus of the present study is to model the detailed wind and tide-induced circulation in Buzzards Bay. The observed tide and current harmonics (Signell, 1987) at stations shown in Fig. 2(a) and the observed surface elevations and currents (Butman et al., 1988) at stations shown in Fig. 2(b) and (c) are used to validate the model predictions. The calibrated model is then used to study the relative contributions of tidal and wind forcing on the instantaneous and residual circulation in Buzzards Bay.

2. Description of the study area and its hydrography

Buzzards Bay communicates with the Rhode Island Sound through its mouth, with Vineyard Sound through Woods Hole and Quicks Hole, and with Cape Cod Bay through the Cape Cod Canal. The bay is 40 km long, and varies in width from

10 km near the mouth to a maximum of 20 km near New Bedford. More details about the bay and its formation during last ice age can be found in Signell (1987). Buzzards Bay is quite shallow (Fig. 1) with a mean depth of 11 m at Mean Low Water (MLW). Mean depths at MLW vary from 5 to 10 m, near the head to 20 m near the mouth.

Currents within Buzzards Bay are dominated by semi-diurnal M_2 tides, with the amplitudes of tidal currents decreasing from a maximum of 50–60 cm/s near the mouth to 10–15 cm/s at the head (Signell, 1987). The currents in Vineyard Sound range from 70 to 100 cm/s (Haight, 1938). The large phase and amplitude difference between Buzzards Bay and Vineyard Sound leads to extremely large currents in Woods Hole and Quicks Hole.

The annual average fresh water volume flux into Buzzards Bay was calculated to be $15.0 \text{ m}^3/\text{s}$ (Signell, 1987). Salinities generally range between 30 and 32 psu, with annual variations of less than 1 psu (Rosenfield et al., 1984). Buzzards Bay is well mixed during October–February, but vertical stratification could develop during spring and summer due to surface heat flux. Signell (1987) calculated the estuarine circulation in Buzzards Bay to be 1 cm/s, based on a simple, static, frictional model in which along the bay pressure gradient is balanced by the divergence of vertical stress.

3. Model description

The hydrodynamic model used in the present study is the three-dimensional time-dependent generalized non-orthogonal boundary-fitted model in spherical coordinates developed by

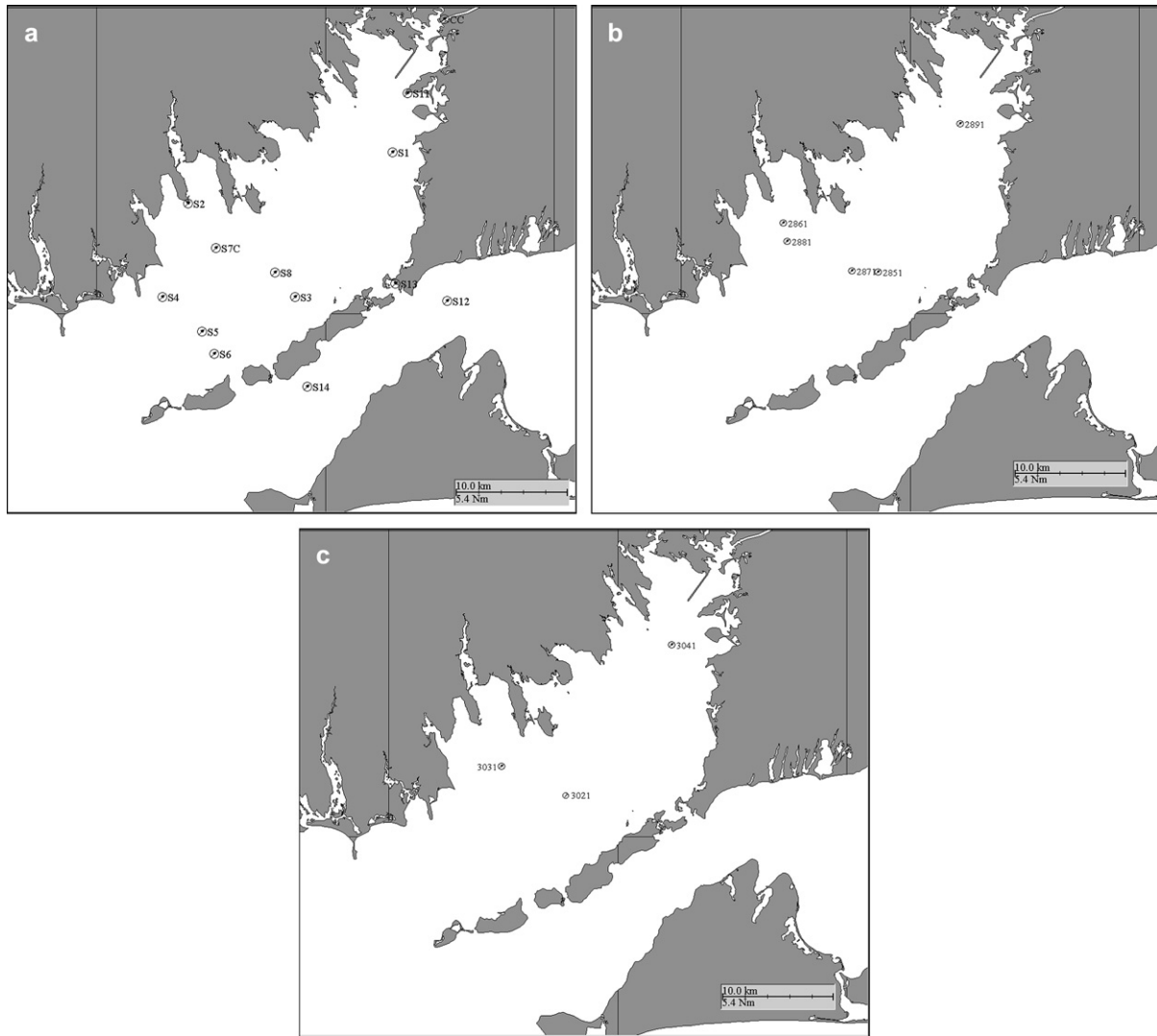


Fig. 2. (a) Location of tide gauge and current measurement stations given in Signell (1987) in Buzzards Bay and Vineyard. (b) Location of tide gauge stations in Buzzards Bay during August–December 1984 (Butman et al., 1988). (c) Location of current meter stations in Buzzards Bay during August–December 1985 (Butman et al., 1988).

Muin and Spaulding (1997a). This model, called BFHYDRO (Boundary-Fitted Hydrodynamic model), has been successfully applied to coastal and estuarine waters. Some recent applications for the model include the Mount Hope Bay (Swanson et al., in press), Providence River (Muin and Spaulding, 1997b), and bay of Fundy (Sankaranarayanan and French McCay, 2003). The model solves a coupled system of partial differential equations describing conservation of mass, momentum, salt and temperature, in a generalized non-orthogonal boundary-fitted coordinate system. An orthogonal coordinate version of the model (Sankaranarayanan and Ward, 2006) was recently applied to study the three-dimensional circulation in Narragansett Bay. The equations of continuity and motion on a spherical coordinate system are given below.

Continuity Equation

$$\frac{1}{r \cos \theta} \frac{\partial u}{\partial \phi} + \frac{1}{r} \frac{\partial v}{\partial \theta} - \frac{v}{r} \tan \theta + \frac{1}{r^2} \frac{\partial r^2 w}{\partial r} = 0 \quad (1)$$

Momentum equation in ϕ -direction

$$\begin{aligned} \frac{\partial u}{\partial t} + \frac{u}{r \cos \theta} \frac{\partial u}{\partial \phi} + \frac{v}{r} \frac{\partial u}{\partial \theta} - \frac{uv}{r} \tan \theta + w \frac{\partial u}{\partial r} + \frac{uw}{r} - fv \\ = -\frac{1}{\rho_0 r \cos \theta} \frac{\partial p}{\partial \phi} + \frac{\partial}{\partial r} \left(A_v \frac{\partial u}{\partial r} \right) \end{aligned} \quad (2)$$

Momentum equation in θ -direction

$$\begin{aligned} \frac{\partial v}{\partial t} + \frac{u}{r \cos \theta} \frac{\partial v}{\partial \phi} + \frac{v}{r} \frac{\partial v}{\partial \theta} - \frac{uv}{r} \tan \theta + w \frac{\partial v}{\partial r} + \frac{vw}{r} + fu \\ = -\frac{1}{\rho_0 r} \frac{\partial p}{\partial \theta} + \frac{\partial}{\partial r} \left(A_v \frac{\partial v}{\partial r} \right) \end{aligned} \quad (3)$$

Momentum equation in r -direction

$$\frac{\partial p}{\partial r} = -\rho_0 g \quad (4)$$

where ϕ is the longitude positive east; θ is the latitude positive north; r is the radius of earth; u and v are the three-dimensional

velocities in (ϕ, θ) directions, respectively; f is the Coriolis parameter; g is the gravity; ρ_0 is the reference density; and A_v is the vertical eddy viscosity.

Eqs. (1)–(4) are transformed to a σ -coordinate system on the vertical plane and a generalized non-orthogonal coordinate system on the horizontal plane. The fully transformed equations are given in Muin and Spaulding (1997a).

Boundary conditions:

$$\begin{aligned} \text{At the surface } \sigma = 0, \quad & \frac{A_v}{D} \left(\frac{\partial u}{\partial \sigma}, \frac{\partial v}{\partial \sigma} \right) \\ & = \gamma_s \left(\sqrt{W_\phi^2 + W_\theta^2} \right) (W_\phi, W_\theta) \end{aligned} \quad (5)$$

$$\begin{aligned} \text{At the bottom } \sigma = -1 \quad & \frac{A_v}{D} \left(\frac{\partial u}{\partial \sigma}, \frac{\partial v}{\partial \sigma} \right) \\ & = C_d \left(\sqrt{u_b^2 + v_b^2} \right) (u_b, v_b) \end{aligned} \quad (6)$$

where c_d is the quadratic bottom drag coefficient, γ_s is the surface wind stress coefficient, u_b and v_b are the velocities at the bottom sigma level, and W_ϕ and W_θ are the wind speeds respectively, in ϕ - and θ -directions.

The vertical boundary conditions are

$$\omega = 0 \text{ at } \sigma = 0 \text{ and } \sigma = -1 \quad (7)$$

At the land boundaries, the normal component of the velocity is set to zero. At the open boundaries, the water surface elevation is specified as a function of time. The river boundaries are given by a specified inflow-velocity and horizontal pressure gradient is set to zero.

The equations of motion (Eqs. (1)–(3)) is split into exterior and interior modes to increase the allowable time step and hence reduce the computational time. Solution of the exterior mode using a semi-implicit solution methodology has been described by Muin and Spaulding (1996). The vertical diffusion term for the interior mode is solved implicitly using a three-time level scheme. The spatial discretization is based on a space staggered C-grid system (Arakawa and Lamb, 1977) and the temporal discretization is based on three-time level scheme with a weighting factor of 1.5. Thus the algorithm is second order accurate in time and space. The boundary-fitted model technique matches the model coordinates with the shoreline boundaries and allows the user to adjust the model grid resolution as desired.

The boundary-fitted grid for the study area is shown in Fig. 3. The grid is composed of 17 232 curvilinear elements in the horizontal, and 11 equal sigma levels in the vertical plane. The grid resolution ranges from about 500 m near the mouth of the Buzzards Bay to about 150 m in the center of the bay.

4. Model forcing functions

Buzzards Bay is well mixed during October–February, but vertical stratification could develop during spring and summer due to surface heat flux and the present study does not account this into account. Signell (1987) calculated the estuarine circulation in Buzzards Bay to be 1 cm/s, based on a simple static, frictional model in which along the bay pressure gradient is balanced by the divergence of vertical stress. In the present study, the density is assumed to be constant and the effects of stratification due to variation in salinity and temperature are not taken into account. The open boundaries were forced

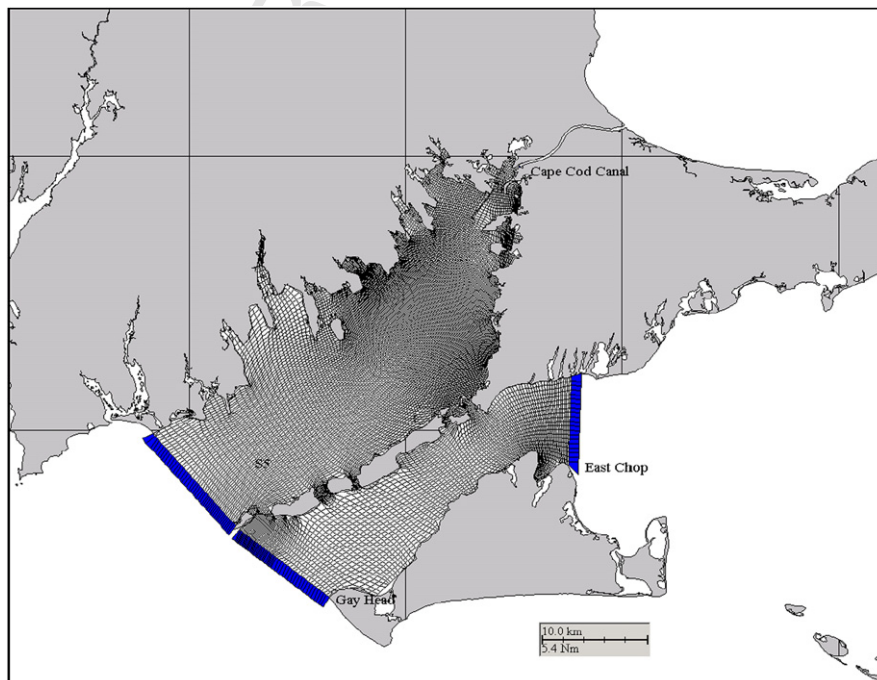


Fig. 3. Boundary-fitted grid for the study area.

with elevations, calculated from a harmonic composition of tidal constituents and then added to the low-frequency elevations obtained from observations by Butman et al. (1988). The details about the wind forcing on the surface and forcing along the open boundaries are given in the following sections. All the simulations presented in this study are conducted during the months of August–December.

4.1. Tidal elevations

The study area consists of three open boundaries: (a) along the mouth of the bay, (g) across Vineyard Sound near East Chop, and (c) across Cape Cod Canal at the Buzzards Bay entrance (Fig. 3). Surface elevations forced along the open boundaries were obtained from a harmonic composition (Foreman, 1978) of tidal constituents (Tables 1 and 2) given by National Ocean Service (NOS) and Signell (1987). Harmonic constants along the mouth of Buzzards Bay were obtained from a linear interpolation of amplitudes and phases at Gay Head (NOS) and at Station S5 (Table 2) from Signell (1987).

4.2. Winds

The wind speeds from Buzzard Bay Buoy (BUZM3) recorded at an anemometer height of 24.8 m, obtained from the National Data Buoy Center were transformed to wind speeds at 10 m elevation, using Prandtl 1/7 law approximation to the logarithmic velocity profile such that,

$$\frac{W_{10}}{W_z} = \left(\frac{10}{z}\right)^{1/7} \quad (8)$$

where z is the anemometer height, and W_{10} and W_z are the wind speeds, respectively, at 10 m and z m heights. The logarithmic approximation is more accurate and universal, but the 1/7 law approximation (Streeter et al., 1998) is more convenient to apply and commonly use (Kamphuis, 2001; Resio et al., 2002). Fig. 4 shows the wind speeds from the BUZM3 Buoy, corrected for the anemometer height. A comparison of the wind speeds at New Bedford Airport and Buzzards Bay Buoy, BUZM3 showed that the wind speeds at Buzzards Bay are higher by a factor of 1.5. Since it is well known that airport winds on land are smaller than winds over the ocean, especially at night and stable conditions, it was decided to use the winds from Buzzards Bay Buoy corrected for 10 m height, for model wind forcing in the present study. The observed winds from Buzzards Bay (BUZM3) during August 20, 1985–December 3, 1985 were used for model wind forcing to compare the model-predicted wind-induced currents with observations from Butman et al. (1988).

4.3. Low-frequency elevations

The observed sea surface pressures in Buzzards Bay reported in Butman et al. (1988) and available at http://stellwagen.er.usgs.gov/buzz_bay-1h.html were first used to study the variation in low-frequency surface elevations in Buzzards

Table 1
Harmonics of major tidal constituents at Gay Head and S5

Constituent	Gay Head (NOS)		S5 (Signell, 1987)	
	Amp (m)	Phase (°)	Amp (m)	Phase (°)
M_2	0.425	226.6	0.506	218.7
N_2	0.109	210.7	0.121	195.0
S_2	0.089	236.8	0.131	235.2
K_1	0.063	110.1	0.068	104.2
O_1	0.047	126.9	0.057	121.8
M_4	0.037	90.0	0.063	103.9

Bay. The observed sea surface pressures were converted to sea surface elevations, taking 1 mbar = 0.995 cm close to the water surface. The observed surface elevations at Woods Hole from NOAA for the same period were obtained from <http://tidesandcurrents.noaa.gov>. The low-frequency fluctuations in surface elevations were obtained from the hourly surface elevations using a fifth-order, 32-h low-pass Butterworth filter. The phase shift inherent in the Butterworth filter is removed by passing the data backward and forward through the filter. The low-frequency elevations at Stations 2851 and 2861 (Fig. 5, top panel) are well correlated with a high correlation coefficient of 0.983. The low-frequency elevations at Stations 2871 and 2891 (Fig. 5, bottom panel) are also well correlated with a high correlation coefficient of 0.990. Thus, the observed low-frequency elevations do not show much variation (Fig. 5) in Buzzards Bay. Table 3 gives correlation coefficients between the observed low-frequency elevations at Buzzards Bay. It is noted that the low-frequency elevations at stations in Buzzards Bay are not well correlated with low-frequency elevations in Woods Hole, with correlation coefficients less than 0.621.

Although surface elevation data were available during September–December 1984 from Butman et al. (1988), the wind observations from the Buzzards Bay at BUZM3 were available only from August 1985. The observed wind records from the Buzzards Bay BUZM3 during August 20, 1985–December 3, 1985 were available with a corresponding period of availability for surface elevation observations at Station 3021, during August 20, 1985–December 3, 1985.

5. Skill assessment of the model

The harmonic constants for surface elevations at Woods Hole and New Bedford, obtained from NOS, and the harmonic constants for surface elevations at eight stations and currents at

Table 2
Harmonics of major tidal constituents at Cape Cod Canal and East Chop

Constituent	Cape Cod Canal (NOS)		East Chop (NOS)	
	Amp (m)	Phase (°)	Amp (m)	Phase (°)
M_2	0.507	267.6	0.244	330.2
N_2	0.155	244.5	0.061	297.8
S_2	0.087	270.4	0.034	350.3
K_1	0.106	120.1	0.035	136.0
O_1	0.079	117.7	0.024	111.1
M_4	0.081	132.6	0.015	41.2

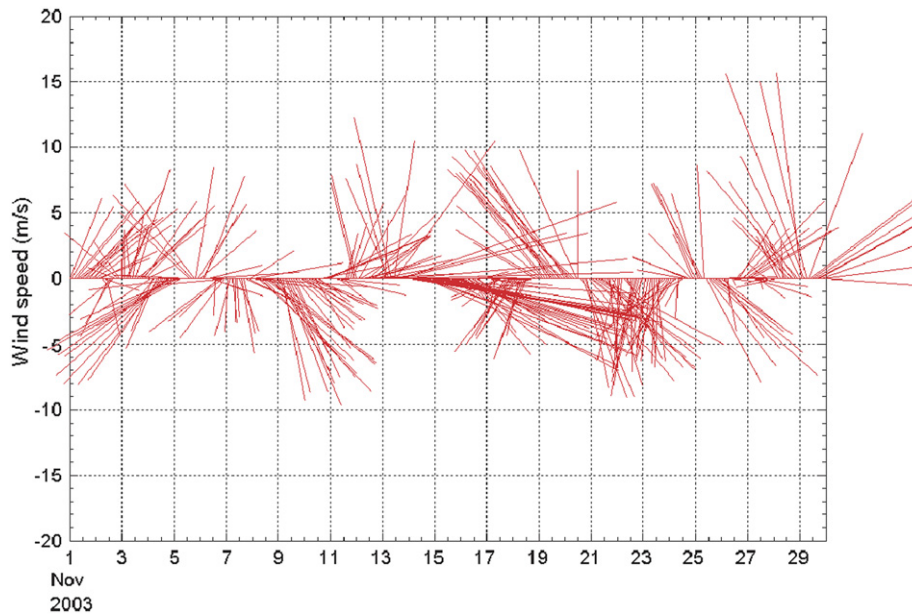


Fig. 4. Observed wind records at Buzzards Bay Buoy (BUZM3) during November 2003.

seven stations (Fig. 2a) given in Signell (1987) are used to calibrate the model predictions. The observed surface elevations and currents given in Butman et al. (1988) are used to validate the model-predicted low-frequency surface elevations and currents. Time series of surface elevations at Woods Hole obtained from NOS are also used to evaluate the model predictions.

5.1. Tidal surface elevations

The model amplitudes and phases of the major tidal constituents were obtained from a harmonic analysis (Foreman,

1978) of model surface elevation data from the 60-day simulation, during November–December 2003. The quadratic bottom friction coefficient was varied between 0.002 and 0.006 to match the model-predicted amplitudes and phases with the observations. Comparison of the errors in the amplitudes and phases showed that best match to observations was obtained using a bottom friction coefficient of 0.003. A comparison of the predicted harmonic amplitudes and phases with the observations at Woods Hole and New Bedford, respectively, are given in Tables 4 and 5. It is seen that the error in amplitudes for the major tidal constituents are less than 4 cm at these two stations. The errors in the phases for the dominant

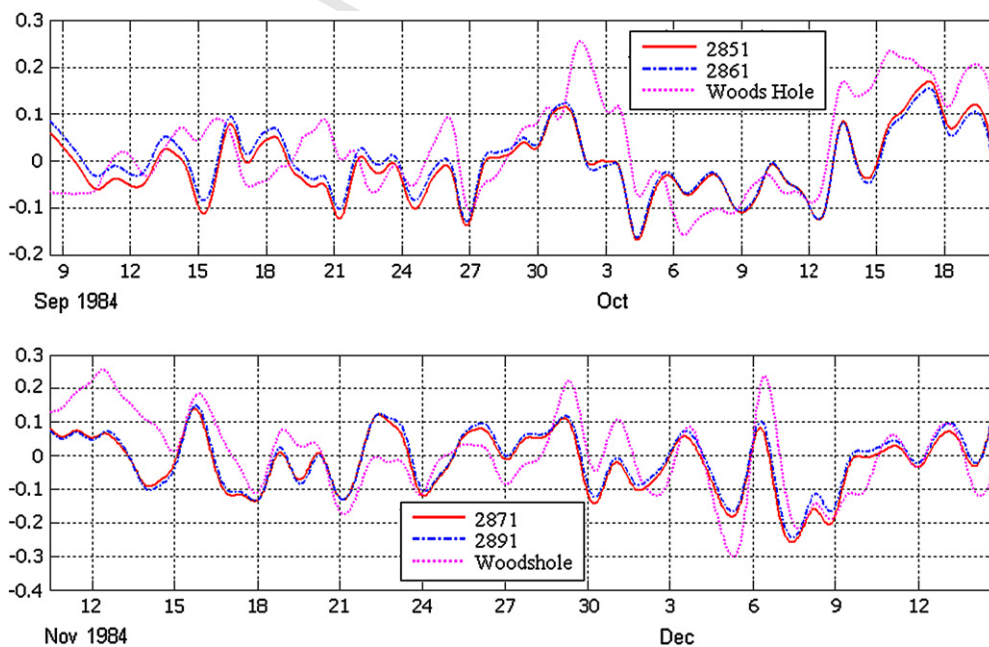


Fig. 5. Comparisons of observed low-frequency surface elevations at stations in Buzzards Bay (Butman et al., 1988) and Woods Hole (NOAA).

Table 3
Comparison of low-frequency surface elevations at stations in Buzzards Bay (Butman et al., 1988) with NOAA observations at Woods Hole

Station	Correlation with observations at Woods Hole
2851	0.621
2861	0.544
2871	0.619
2891	0.593

semi-diurnal constituents are less than 8° . The errors in the predicted phases for the other harmonic constituents are slightly higher, but their effects are small when compared with M_2 . A comparison of the predicted and observed M_2 tidal harmonic constituents (Signell, 1987) at eight stations (Fig. 2a) is given in Table 6. The errors in the predicted amplitudes and phases are, respectively, within 2 cm and 5° .

5.2. Low-frequency surface elevations

A comparison of low-frequency surface elevations at station at Woods Hole is shown in Fig. 6. The RMS error in low-frequency surface elevation between observations and the model predictions at Woods Hole is 0.075 m during the period August 21–December 31, 1985. The model-predicted low-frequency surface elevations at Woods Hole closely follow the trends seen in the observations with a correlation coefficient of 0.735, but fail to capture some of the peak surges seen in the observations. The model-predicted surface elevations at stations inside Buzzards Bay do not show much variation, as reflected in the observations (Fig. 5).

5.3. Tidal currents

Tidal current harmonics for the model-predicted currents for a 60-day period (November–December, 2003) were performed using the package T_tide (Pawlowicz et al., 2002). A constant vertical eddy viscosity of $0.050 \text{ m}^2/\text{s}$ was used. The model-predicted M_2 harmonic principal current speeds and directions (Table 7) in Buzzards Bay showed good comparison with observations (Signell, 1987) at all seven stations. The errors in the model-predicted M_2 principal current speeds are less than 6 cm/s. The model-predicted principal current

Table 4
Comparison of observed (NOS) and predicted tidal harmonic amplitudes and local phases for different tidal constituents at Woods Hole

Constituent	Observed amplitude (m)	Predicted amplitude (m)	Deviation (m)	Observed Phase ($^\circ$)	Predicted phase ($^\circ$)	Deviation ($^\circ$)
M_2	0.235	0.248	-0.013	250.8	254.1	-3.3
N_2	0.059	0.059	0.000	246.7	254.5	-7.8
S_2	0.077	0.066	0.011	238.7	234.3	4.4
K_1	0.072	0.054	0.018	114.8	122.4	-7.6
O_1	0.066	0.043	0.023	132.6	116.3	16.3
M_4	0.055	0.036	0.019	66.0	88.6	-22.6

Table 5
Comparison of observed (NOS) and predicted tidal harmonic amplitudes and local phases for different tidal constituents at New Bedford

Constituent	Observed amplitude (m)	Predicted amplitude (m)	Deviation (m)	Observed Phase ($^\circ$)	Predicted phase ($^\circ$)	Deviation ($^\circ$)
M_2	0.536	0.498	0.038	218.6	221.5	-2.9
N_2	0.130	0.131	0.001	234.6	234.5	0.1
S_2	0.137	0.118	0.019	206.4	202.1	4.3
K_1	0.062	0.071	-0.009	95.2	111.1	-15.9
O_1	0.049	0.061	-0.012	128.8	117.1	11.7
M_4	0.078	0.067	0.011	107.7	105.7	2.0

directions and phases are within 14° of the observations and the minor axis currents are very small in the bay, except at the head of the bay (Table 8). The model-predicted tidal ellipse parameters for the N_2 , S_2 , and M_4 harmonic constituents also showed good comparison with the observations (not given here).

Table 9 shows a comparison of observed (based on a 1931 survey) and model-predicted M_2 tidal current amplitudes and phases at Woods Hole and Quicks Hole. The errors in the model-predicted current amplitudes are less than 3% and the model-predicted phases are within 10° of the observations.

5.4. Low-frequency currents

The observed currents in Buzzards Bay at Stations 3021, 3031, and 3041 (Butman et al., 1988) during August–December 1985 were obtained from the hourly current observations available at http://stellwagen.er.usgs.gov/buzz_bay-a1h.html. The low-frequency currents were obtained from the hourly observations using a fifth-order, 32-h low-pass Butterworth filter. The phase shift inherent in the Butterworth filter is removed by passing the data backward and forward through the filter. The model-predicted low-frequency currents in the east–west direction at Stations 3021, 3031, 3041 compare well with the observations as shown in the top panel in Fig. 7(a)–(c) with the model capturing the trends seen in the observations, for the most part. However, the model-predicted north–south velocities do not compare well with

Table 6
Comparison of observed (Signell, 1987) and predicted tidal harmonic amplitudes and local phases for M_2 tidal constituent in Buzzards Bay

Station	Observed amplitude (m)	Predicted amplitude (m)	Deviation (m)	Observed Phase ($^\circ$)	Predicted phase ($^\circ$)	Deviation ($^\circ$)
S1	0.531	0.528	0.003	220.4	225.1	-4.7
S2	0.513	0.498	0.015	222.7	221.5	1.2
S5	0.506	0.507	-0.001	218.7	223.3	-4.6
S7	0.507	0.498	0.009	222.1	221.8	0.3
S8	0.505	0.507	-0.002	220.7	223.1	-2.4
S11	0.551	0.540	0.011	226.4	225.8	0.6
S12	0.554	0.537	0.017	226.7	226.7	0.0
S13	0.228	0.231	-0.003	251.3	256.3	-5.0

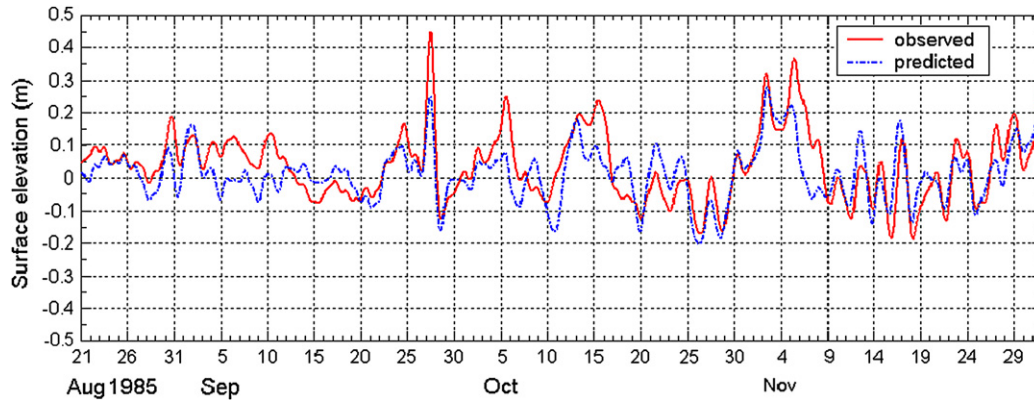


Fig. 6. Comparisons of observed and predicted low-frequency surface elevations at Woods Hole.

the observations. The addition of low-frequency surface elevations at station 3021 for the elevation forcing at the open boundaries did not improve the model-predicted low-frequency currents. Table 10 shows statistical comparisons of observed (Butman et al., 1988) and predicted low-frequency currents at three stations in Buzzards Bay. The lack of good performance in the model-predictions for one of the components of the low-frequency velocities was reported for the modeling studies in New York Harbor (Sankaranarayanan, 2005) and Narragansett Bay (Sankaranarayanan and Ward, 2006). The lack of good skill in the model-predicted low-frequency currents in the north–south direction can be attributed to the fact that the circulation due to non-local forcing is not taken into account in the present study, since the model is forced with only clamped elevations along the open boundaries.

6. Tide-induced circulation

Fig. 8(a) and (b) shows, respectively, the model-predicted depth-averaged tidal currents during peak flood and peak ebb, with the peaks referenced with respect to Station S8 (Fig. 2a), located at the center of the bay. The depth-averaged tidal currents at peak flood range from 30 to 60 cm/s in Buzzards Bay, from 60 to 90 cm/s in Vineyard Sound, from

Table 7 Comparison of observed and predicted M₂ harmonic principal current speeds and directions in Buzzards Bay

Station	Depth from MSL (m)	Principal current speed (cm/s)			Principal current direction (°T)		
		Obs.	Model	Error	Obs.	Model	Error
S4	5	25.7 ± 0.4	30.0	-4.3	39.9 ± 1.0	42.0	-2.1
S4	10	22.1 ± 0.5	28.2	-6.1	36.2 ± 1.4	42.0	-5.8
S5	5	24.9 ± 0.7	27.9	-3.0	75.0 ± 1.4	69.9	5.1
S5	10	21.5 ± 0.7	25.7	-4.2	70.8 ± 1.6	69.8	1.0
S6	5	22.5 ± 0.5	28.5	-6.0	75.9 ± 1.2	78.0	-2.1
S6	10	21.4 ± 0.8	26.3	-4.9	72.7 ± 2.2	78.0	-5.3
S1	12	9.5 ± 0.5	11.6	-2.1	14.0 ± 3.2	22.4	-8.4
S7	9	12.4 ± 0.5	14.0	-1.6	44.3 ± 2.4	57.8	-13.5
S8	15	13.3 ± 0.6	18.1	-4.8	45.2 ± 2.4	59.2	-14.0
S14	Depth averaged	75.3 ± 1.1	72.4	2.9	55.8 ± 0.8	55.5	0.3

1.2 to 2.7 m/s near Woods Hole, and from 0.9 to 1.2 m/s near Quicks Hole. The tidal currents flow from Buzzards Bay into Vineyard Sound through the Holes (Woods Hole and Quicks Hole) during flooding and from Vineyard Sound into Buzzards Bay through the Holes during ebbing, with flood currents being more dominant at the Holes. The model predictions agree with the observations that tidal currents in Vineyard Sound lagged the currents in Buzzards Bay by more than 3 h. Observed M₂ tidal harmonic current phase at Station S14 in Vineyard Sound lags the currents at Station S3 in Buzzards Bay (Table 8) by 88° (about 3 h).

7. Wind-induced circulation

Local winds often play a dominant role in the circulation in bays and estuaries. Csanady (1974) showed that the interaction of wind stress with bathymetric gradients generates vortex currents, using the vorticity equation for vertically averaged flow. Neglecting bottom friction, Csanady (1974) derived the linearized vorticity equation to be

$$\frac{d}{dt} \left(\frac{\eta + f}{h + \zeta} \right) = \frac{1}{h + \zeta} \left[\frac{\partial}{\partial x} \left(\frac{\tau_s^y}{\rho h} \right) - \frac{\partial}{\partial y} \left(\frac{\tau_s^x}{\rho h} \right) \right] \quad (9)$$

Table 8 Comparison of M₂ harmonic tidal current phases and minor axis currents in Buzzards Bay

Station	Depth from MSL (m)	Principal current Phase (°)			Minor axis speed (cm/s)		
		Obs.	Model	Error	Obs.	Model	Error
S4	5	151.5 ± 1.0	154.2	-2.7	-0.6 ± 0.5	0.0	-0.6
S4	10	151.2 ± 1.2	153.7	-2.5	-0.6 ± 0.5	0.0	-0.6
S5	5	167.3 ± 1.6	165.8	1.5	-4.9 ± 0.6	-4.7	-0.2
S5	10	165.3 ± 2.0	165.1	0.2	-3.9 ± 0.6	-4.4	0.5
S6	5	161.3 ± 1.4	169.2	-7.9	-4.5 ± 0.4	-6.3	1.8
S6	10	161.0 ± 2.4	168.5	-7.5	-4.3 ± 0.7	-6.1	1.8
S1	12	152.3 ± 3.2	159.8	-7.5	0.8 ± 0.5	0.2	0.6
S7	9	142.8 ± 2.6	153.2	-10.4	0.3 ± 0.5	-3.0	3.3
S8	15	147.8 ± 2.4	160.7	-12.9	0.6 ± 0.6	-1.6	2.2
S14	Depth averaged	239.1 ± 0.8	239.2	-0.1	2.3 ± 1.0	3.4	-1.1

Table 9

Comparison of observed and model-predicted M_2 tidal current amplitudes and phases at Woods Hole and Quicks Hole

Station	Latitude	Longitude	Principal current speed (cm/s)			Phase (°)		
			Obs.	Model	Error	Obs.	model	error
Woods Hole	-70.6850	41.5200	174.8	169.5	5.3	212.9	211.8	1.1
Quicks Hole	-70.8483	41.4433	114.7	115.5	-0.8	219.9	208.9	11

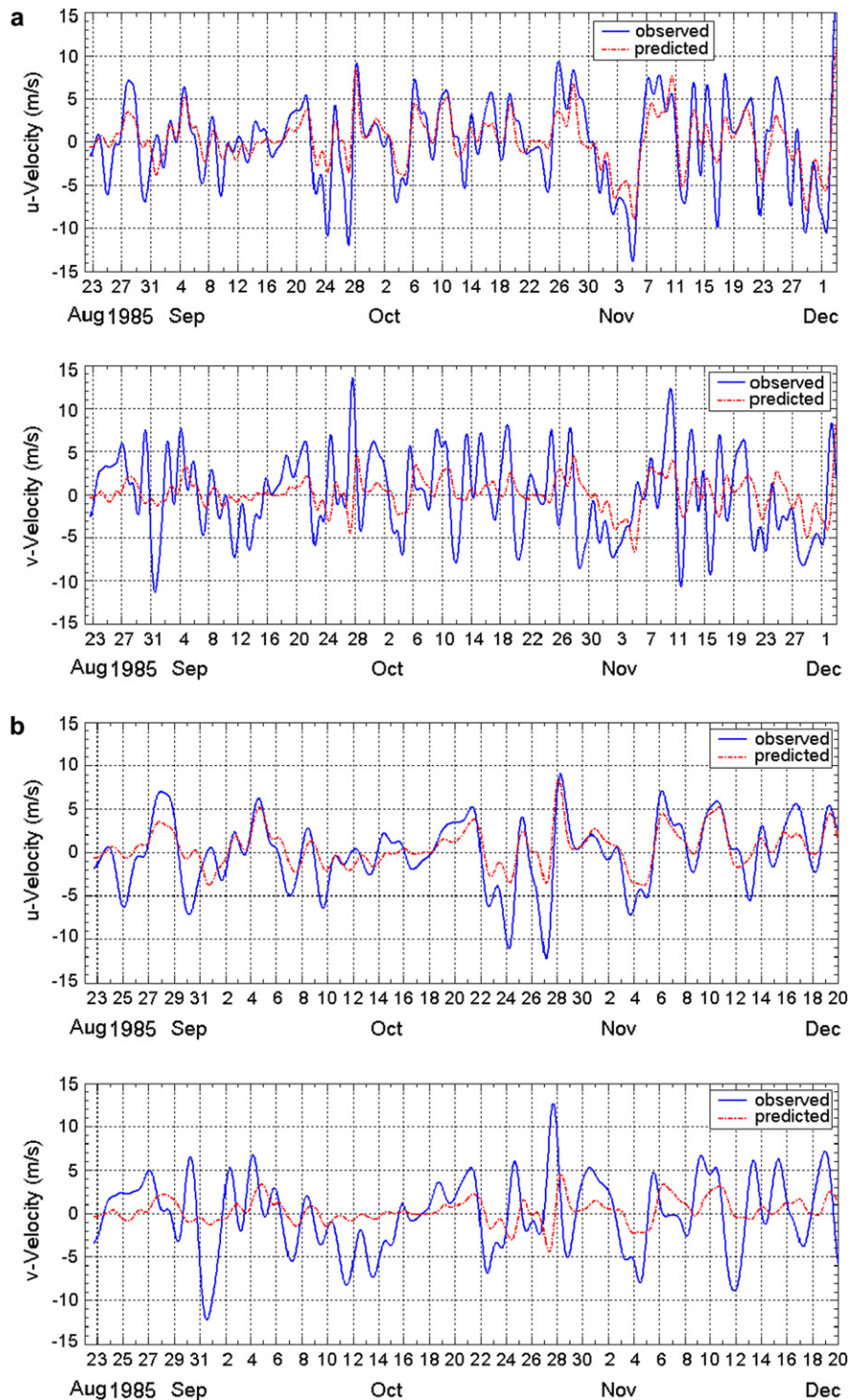


Fig. 7. (a) Comparison of observed (Butman et al., 1988) and model-predicted east–west and north–south velocities at Station 3021. (b) Comparison of observed (Butman et al., 1988) and model-predicted east–west and north–south velocities at Station 3031. (c) Comparison of observed (Butman et al., 1988) and model-predicted east–west and north–south velocities at Station 3041.

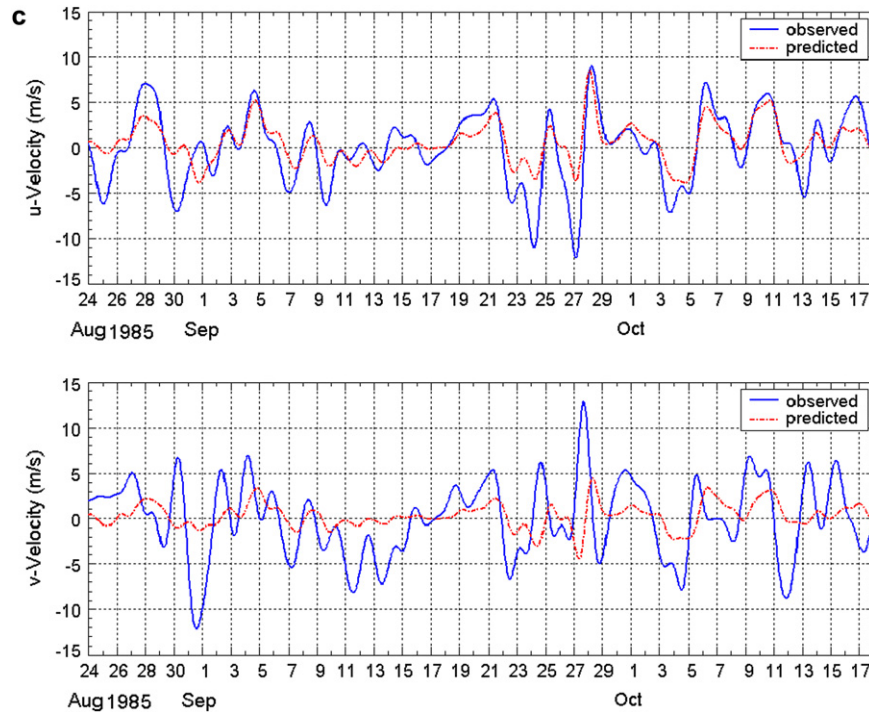


Fig. 7 (continued).

where $\eta = (\partial v / \partial x) - (\partial u / \partial y)$ is the relative vorticity. It can be seen from Eq. (9) that vorticity changes can occur due to changes in sea surface elevation, water depth and curl of the wind stress. Csanady (1974) suggested that the double gyre circulation in Gulf of Maine is due to the barotropic response to northeasterly wind stress, using the depth-averaged vorticity equation and observations. It should be noted that Csanady's theory explains the directional sense of gyres, caused due to wind forcing, but does not explain the size and shape of the gyres.

7.1. Depth-averaged wind-induced currents during November 2003

Fig. 9 shows the model-predicted depth-averaged wind-induced currents in Buzzards Bay due to strong winds from the northeast direction. The model-predicted wind-induced currents in Buzzards Bay are in the same direction as the wind, with speeds up to 20 cm/s in the shallow water, and in the opposite direction to the winds, with speeds up to 6 cm/s

Table 10
Statistical comparisons of observed (Butman et al., 1988) and model-predicted low-frequency velocities

Station	Number of data points	RMS error (cm/s)		Correlation coefficient	
		East velocity	North-velocity	East velocity	North-velocity
3021	2071	2.67	4.38	0.852	0.276
3031	1399	2.50	4.10	0.817	0.244
3041	1321	2.54	4.14	0.811	0.207

in the deep water. The model-predicted wind-induced currents in Vineyard Sound are in the same direction as the wind, with speeds up to 30 cm/s. The model-predicted wind-induced current speeds through Woods Hole flowing into Buzzards Bay reach as high as 50 cm/s, while the currents through Quicks Hole, flowing into Buzzards Bay, reach as high as 40 cm/s. The prominent vortices 1 through 4 generated due to winds from the northeast, labeled in Fig. 9, can be explained using Eq. (9). An increasing depth to the right of a wind blowing parallel to the coast causes a clock-wise gyre (labeled 3 and 4 in Fig. 9, while a decreasing depth to the right of the wind causes an anti-clockwise gyre (labeled 1 and 2 in Fig. 9).

Fig. 10 shows the model-predicted depth-averaged wind-induced circulation pattern due to strong winds blowing from the southwest direction on November 29. The two anti-clockwise vortices (labeled 1 and 2) and three clock-wise vortices (labeled 3, 4, and 5) can also be explained using Eq. (9). The wind-induced currents due to winds from the southeast, flow from Buzzards Bay into Vineyard Sound through Woods Hole and Quicks Hole. Although directional sense of the model-predicted eddies agree with the theory outlined in Csanady (1974), the size and shape of the eddies obtained from the model need to be validated.

8. Residual currents in Buzzards Bay

Residual currents could be generated due to non-linearity in the dynamics of tidal flow (Signell and Geyer, 1991) local wind stress on the surface (Rady et al., 1998), longitudinal density gradient (Weisberg and Sturges, 1976). The magnitudes

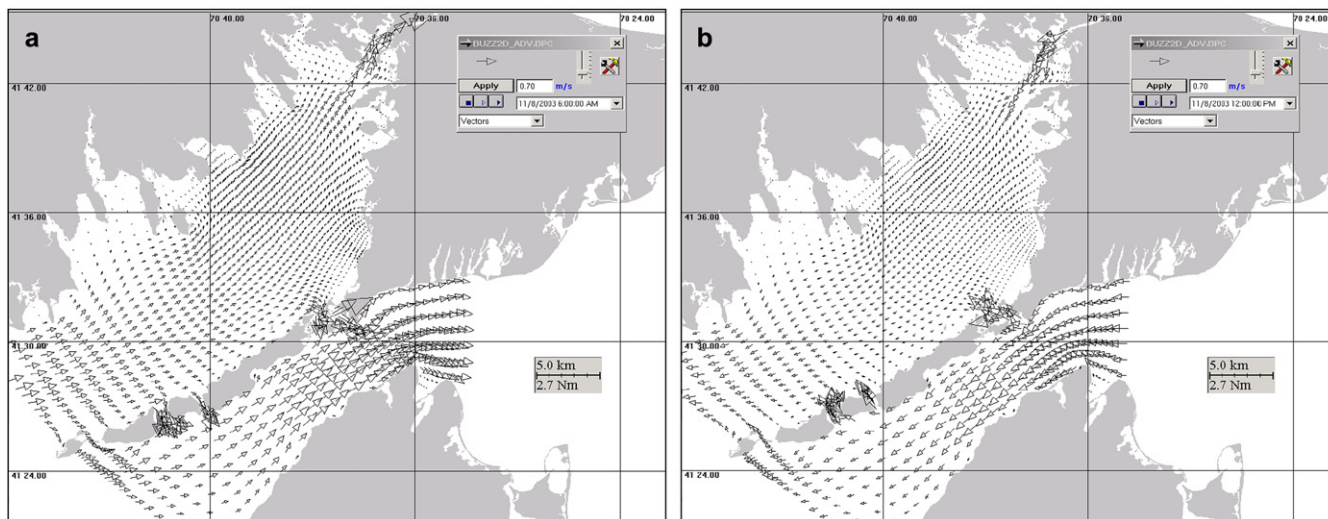


Fig. 8. (a) Model-predicted depth-averaged currents at high flood. (b) Model-predicted depth-averaged currents at high ebb.

of the residual current speeds are usually smaller than the tide and wind-induced currents. The model-predicted residual currents presented in this study were obtained by taking a time-average of the model-predicted instantaneous currents, over at least one-month period.

The model-predicted tide induced residual currents were less than 1 cm/s in Buzzards Bay, with maximum residual current speeds of 2 cm/s seen in Vineyard Sound, Quicks Hole and Woods Hole. The wind-induced residual current obtained by time averaging the model-predicted wind-induced currents during November 2003 is shown in Fig. 11. The wind-induced

residual current speeds (Fig. 11) in the study area are smaller than the instantaneous wind-induced current speeds (Fig. 10). The model-predicted wind-induced residual current speeds vary between 5 and 10 cm/s in Buzzards Bay, between 10 and 15 cm/s in Vineyard Sound, and between 15 and 20 cm/s through Woods Hole.

9. Summary and conclusions

A three-dimensional tidal hydrodynamic model application to the Buzzards Bay is performed using the three-dimensional

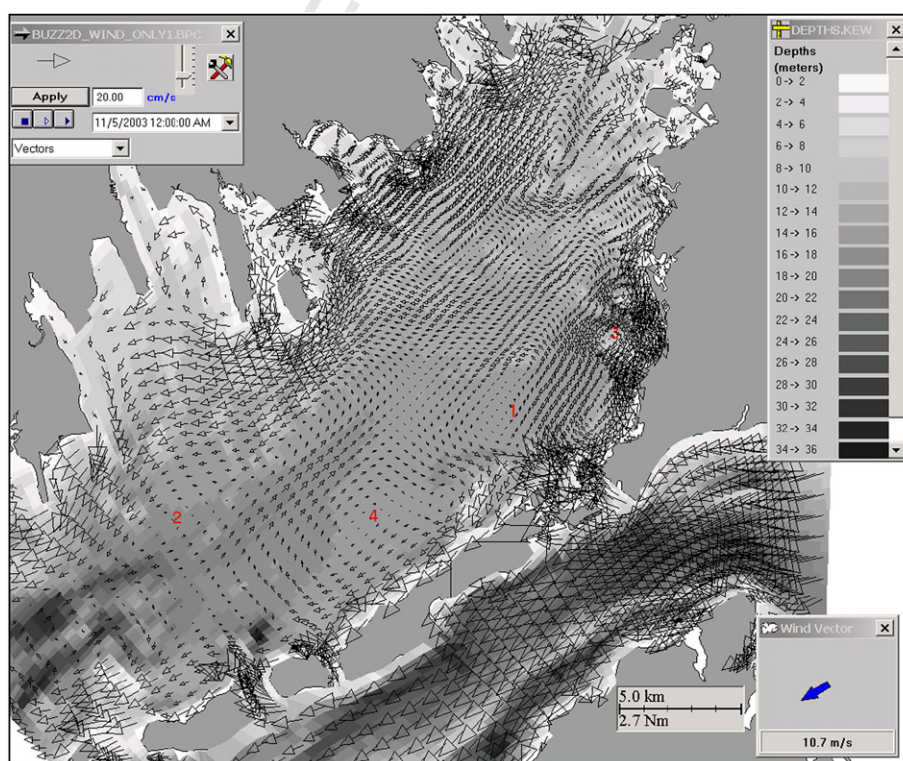


Fig. 9. Wind-induced circulation pattern in Bay on November 5, 2003, 12:00 AM due to strong winds from the northeast direction on November 4.

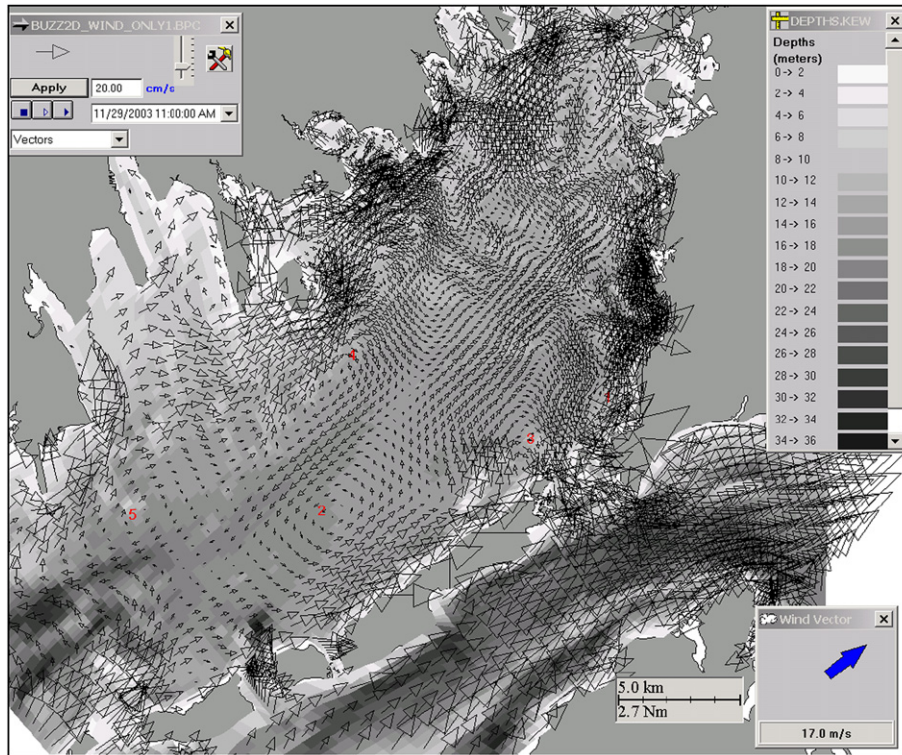


Fig. 10. Wind-induced circulation pattern in Bay on November 29, 2003, 11:00 AM due to strong winds from the southeast direction on November 4.

Boundary-fitted Hydrodynamic model (BFHYDRO). The present study is the first attempt to our knowledge to model the detailed wind and tide-induced circulation pattern in Buzzards Bay and Western Vineyard Sound. The observed surface

elevations and currents given in Butman et al. (1988) and the tide and current harmonics given in Signell (1987) are used to validate the model predictions. The calibrated model is then used to study the relative contributions of tidal and wind

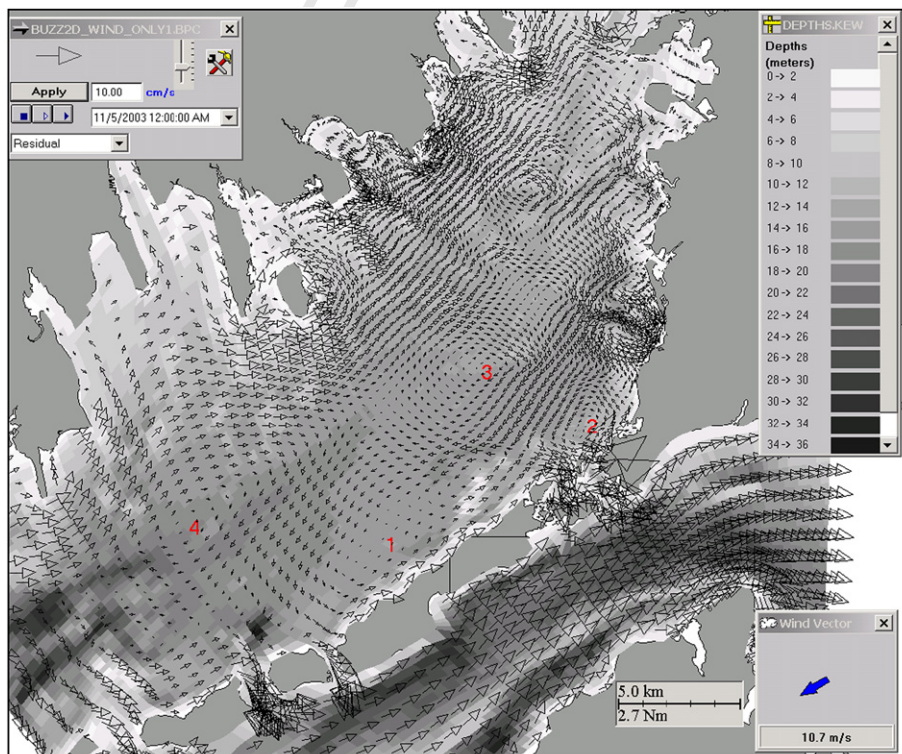


Fig. 11. Wind-induced residual circulation pattern in Buzzards Bay, averaging the model predicted hourly currents over the 30 day period (November 2003).

forcing on the instantaneous and residual circulation in Buzzards Bay.

The model is forced using observed harmonic constants along the open boundaries and winds on the surface. The model predicted surface elevations compare well with the observations, with a high correlation coefficient of 0.92. The amplitudes and phases of the principal tidal constituents at 10 tidal stations in Buzzards Bay obtained from a harmonic analysis of a 60-day simulation compare well with the observed data. The predicted amplitude and phase of the M_2 tidal constituent of surface elevations at these stations are, respectively, within 4 cm and 5° of the observed data. The error in the model-predicted M_2 harmonic principal current speeds are less than 6 cm/s, and the principal current directions and phases are within 14° of the observations.

The model-predicted low-frequency surface elevations at Woods Hole closely follow the trends seen in the observations with a correlation coefficient of 0.735, but fail to capture some of the peak surges seen in the observations. The model-predicted surface elevations at stations inside Buzzards Bay do not show much variation, as reflected in the observations.

The model-predicted M_2 harmonic current speeds and phases at Woods Hole and Quicks Hole also compare well with the observations (based on a 1931 survey). The errors in the model-predicted current amplitudes are less than 3% and the model-predicted phases are within 10° of the observations.

The model-predicted low-frequency currents in the east–west direction at stations in Buzzards Bay compare well with the observations with the correlation coefficient exceeding 0.811 and the model capturing the trends seen in the observations, for the most part. However, the model-predicted north–south velocities do not compare well with the observations. The addition of low-frequency surface elevations for the elevation forcing at the open boundaries did not improve the model-predicted low-frequency currents. The lack of good skill in the model-predicted low-frequency currents in the north–south direction needs to be further investigated, but can be attributed to the fact that the circulation due to non-local forcing is not taken into account in the present study, since the model is forced with only clamped elevations along the open boundaries.

The depth-averaged tidal currents at peak flood range from 30 to 60 cm/s in Buzzards Bay, from 60 to 90 cm/s in Vineyard Sound, from 1.2 to 2.7 m/s near Woods Hole, and from 0.9 to 1.2 m/s near Quicks Hole. The tidal currents flow from Buzzards Bay into Vineyard Sound through the Holes (Woods Hole and Quicks Hole) during flooding and from Vineyard Sound into Buzzards Bay through the Holes during ebbing, with flood currents being more dominant at the Holes.

The model-predicted wind-induced currents in Buzzards Bay are in the same direction as the wind, with speeds up to 20 cm/s in the shallow water, and in the opposite direction to the winds, with speeds up to 6 cm/s in the deep water. The model-predicted wind-induced currents in Vineyard Sound are in the same direction as the wind, with speeds up

to 20 cm/s. The model-predicted wind-induced current speeds through Woods Hole reach as high as 50 cm/s, while the wind-induced current speeds through Quicks Hole, reaching as high as 40 cm/s.

The interaction of wind stress with large bathymetric gradients was shown to cause many vortices in Buzzards Bay, as seen from the model predictions. Model simulations show that the winds play a more dominant role than the tides in the generation of the barotropic residual currents in Buzzards Bay, while the model-predicted tide-induced residual current was seen to be small.

Although directional sense of the model-predicted eddies agrees with the theory outlined in Csanady (1974), the size and shape of the eddies obtained from the model need to be validated.

Uncited reference

Csanady, 1973.

Acknowledgements

The author wishes to thank Bradford Butman of USGS for generously clarifying many points about the field observations conducted by his group in Buzzards Bay during 1982–1986 and making available the data online. The author drew inspiration for writing the paper after attending the Gordon Research Conference on Coastal Ocean modeling in 2003. The author wishes to thank the reviewers for their comments, which helped to significantly improve the manuscript. The author greatly appreciates the efforts by the anonymous reviewer for generously offering many suggestions to improve the work and the manuscript. Encouragement from Paul Hall during the initial modeling effort is also gratefully appreciated.

References

- Arakawa, A., Lamb, V.R., 1977. Computational design of the basic dynamical processes of the UCLA General Circulation Model. *Methods in Computational Physics* 17, 173–265.
- Butman, B., Signell, R., Shoukimas, P., Beardsley, R.C., 1988. Current Observations in Buzzards Bay, 1982–1986. Open File Report 88-5. United States Geological Survey.
- Csanady, G.T., 1973. Transverse internal seiches in large oblong lakes and marginal seas. *Journal of Physical Oceanography* 3, 439–447.
- Csanady, G.T., 1974. Barotropic currents over the continental shelf. *Journal of Physical Oceanography* 4, 357–371.
- Flather, R.A., Heaps, N.S., 1975. Tidal computations for Morecombe Bay. *Geophysical Journal of the Royal Astronomical Society* 42, 489–517.
- Foreman, M.G.G., 1978. *Manual for Tidal Currents and Analysis and Prediction*. Pacific Marine Science, Patricia Bay, Sidney, BC, Canada, 70 pp.
- Haight, P.J., 1938. *Currents in Narragansett Bay, Buzzards Bay, Nantucket and Vineyard Sounds*. Special Publication No. 208. U.S. Government Printing Office.
- Kamphuis, W., 2001. *Introduction to Coastal Engineering and Management*. World Scientific Publishing Company, 472 pp.
- Muin, M., Spaulding, M.L., 1996. Two-dimensional boundary-fitted circulation model in spherical coordinates. *Journal of Hydraulic Engineering* 122 (9), 512–521.

- Muin, M., Spaulding, M.L., 1997a. A 3-D boundary-fitted circulation model. *Journal of Hydraulic Engineering* 123 (1), 2–12.
- Muin, M., Spaulding, M.L., January 1997b. Application of three dimensional boundary fitted circulation model to Providence River. *Journal of Hydraulic Engineering* 123 (1), 13–20.
- Pawlowicz, R., Beardsley, B., Lentz, S., 2002. Classical tidal harmonic analysis including error estimates in MATLAB, using T_TIDE. *Computers and Geosciences* 28, 929–937.
- Rady, M.A., El-Sabah, M.I., Murty, T.S., Backhaus, J.O., 1998. Residual circulation in Gulf of Suez. *Estuarine, Coastal and Shelf Science* 46, 205–220.
- Redfield, A.C., 1953. Interference phenomena in the tides of the Woods Hole region. *Journal of Marine Research* 12, 121–140.
- Resio, D., Bratos, S., Thompson, E., 2002. Meteorology and wave climate. In: Vincent, L., Demirbilek, Z. (Eds.), *Coastal Engineering Manual, Part II, Hydrodynamics*. U.S. Army Corps of Engineers, Washington, DC (Chapter II-2, Engineer Manual 1110-2-1100).
- Rosenfield, L.R., Signell, R.P., Gawarkiewicz, G.G., 1984. Hydrographic Study of Buzzards Bay, 1982–1983. WHOI Tech. Rpt., WHOI-84-5 (CRC-84-01), Woods Hole, MA, 140 pp.
- Streeter, V.L., Wylie, E.B., Bedford, K.W., 1998. *Fluid Mechanics*. McGraw Hill, Singapore, 740 pp.
- Sankaranarayanan, S., French McCay, D., 2003. Three-dimensional modeling of tidal circulation in Bay of Fundy. *ASCE Journal of Waterway, Port, Harbor, Coastal and Ocean Engineering* 129 (3), 114–123.
- Sankaranarayanan, S., Ward, M.C., 2006. Development and application of a three-dimensional orthogonal coordinate semi-implicit hydrodynamic model. *Continental Shelf Research* 26, 1571–1594.
- Sankaranarayanan, S., 2005. A 3D boundary-fitted barotropic hydrodynamic model for the New York Harbor Region. *Continental Shelf Research* 25, 2233–2260.
- Signell, R.P., 1987. Tide- and Wind-forced Currents in Buzzards Bay, Massachusetts. Technical Report WH-87-15. Woods Hole Oceanographic Institution, Woods Hole, Massachusetts.
- Signell, R., Geyer, Rockwell W., 1991. Measurements and modeling of the spatial structure of nonlinear tidal flow around a headland. In: Parker, B. (Ed.), *Tidal Hydrodynamics*. John Wiley & Sons, New York, p. 883.
- Swanson, J.C., Kim, H.S., Sankaranarayanan, S. Modeling of temperature distributions in Mount Hope Bay due to thermal discharges from the Brayton Point Station. *Northeastern Naturalist*, in press.
- Weisberg, R.H., Sturges, W., 1976. Velocity observations in west passage of Narragansett Bay: a partially mixed estuary. *Journal of Physical oceanography* 6, 345–354.